IEEE Access
Multidisciplinary | Rapid Review | Open Access Journal

IEEE POWER & ENERGY SOCIETY SECTION

Received 9 July 2024, accepted 12 August 2024, date of publication 15 August 2024, date of current version 30 August 2024.

Digital Object Identifier 10.1109/ACCESS.2024.3443963

RESEARCH ARTICLE

Dynamic Power Quality Disturbance Classification in Grid-Integrated PV Systems: Leveraging Clark Transformed Modal Voltage and Subspace Weighted KNN

SAIRAM MISHRA[1], (Graduate Student Member, IEEE), RANJAN KUMAR MALLICK[2], (Member, IEEE), PRAVATI NAYAK[1], THAIYAL NAAYAGI RAMASAMY[3], (Senior Member, IEEE), AND GAYADHAR PANDA[4], (Senior Member, IEEE)

[1]Department of Electrical Engineering, Siksha 'O' Anushandhan Deemed to be University, Bhubaneswar, Odisha 751030, India
[2]Department of Electrical and Electronics Engineering, Siksha 'O' Anushandhan Deemed to be University, Bhubaneswar, Odisha 751030, India
[3]Department of Electrical Power Engineering, Newcastle University in Singapore (NUiS), Singapore 567739
[4]Department of Electrical Engineering, National Institute of Technology Meghalaya, Laitumkhrah, Shillong, Meghalaya 793003, India

Corresponding authors: Ranjan Kumar Mallick (rkm.iter@gmail.com) and Thaiyal Naayagi Ramasamy (Naayagi.Ramasamy@newcastle.ac.uk)

The work is funded by Siksha 'O' Anushandhan deemed to be University, Bhubaneswar, Odisha, PIN-751030, India. The research work is carried out by the Microgrid Research Laboratory, Institute of Technical Education and Research. It is also supported by Newcastle University; and in part by the Council of Scientific and Industrial Research (CSIR), Government of India, under Grant 143-2969-9868/2K23/1 (File: 09/0969(18690)/2024-EMR-I).

ABSTRACT This study focuses on detecting Power Quality Disturbance Events (PQDE) in microgrids integrated with a Solar Energy Conversion System (SECS). The research proposes a novel signal reduction technique called Clark Transformed Modal, which reduces three-phase voltage to a single unit signal, optimizing memory utilization and reducing computational load during feature extraction. A total of 16 features are extracted from the proposed modal signal by performing multi-resolution analysis through Maximum Overlap Discrete Wavelet Transform (MODWT). Various disturbances, including sag, swell, transients, notches, and flicker, are intentionally simulated in a PV-grid tied MATLAB/Simulink model to obtain a dataset of 10800 samples. Further, the dataset is randomly divided into training-testing subsets to verify the classification ability of a novel ensemble classifier called subspace weighted k-nearest Neighbor (SWKNN). In addition to that the optimum mother wavelet (dmay) is identified to even further boost the classifier performance. The results demonstrate the superior classification capabilities of the proposed MODWT-SWKNN classifier in terms of various performance metrics like precision, recall and F1-score. It also outperformed when compared with several competitive PQ classification models based on PV-integrated systems both under ideal and noisy conditions. Additionally, the disturbance detection system is validated in an OPAL-RT real-time environment to demonstrate its efficiency in terms of detection time. The accuracy of detection is found to be 99.74% in ideal case and fall back to no more than 3% regulation i.e., 97.28% even in dense noise of 20dB with as low as 8 WKNN subspaces. Further, average detection time with 500 trails is found to be 0.0285 seconds. The efficacy of the proposed PQ detection algorithm is also tested in a large PV integrated IEEE 13-bus system.

INDEX TERMS Clark transform, kth nearest neighbour, maximum overlap discrete wavelet transform, microgrid, power quality classification.

The associate editor coordinating the review of this manuscript and approving it for publication was Shafi K. Khadem.

I. INTRODUCTION

The escalating demand for electricity and a substantial decline in fossil fuel availability in recent decades have prompted the exploration of alternative energy sources to fulfil energy needs. Integrating distributed energy sources, such as Renewable Sources of Energy (RSEs) or traditional synchronous generators, into distribution networks to ensure high-quality power supply has given rise to the concept of micro-grids. Among various RSEs, Solar Energy Conversion System (SECS) has gained notable traction worldwide due to its natural abundance, light weight, and cost-effectiveness [1]. However, SECS also brings a series of challenges such as intermittency, inverter interaction, on/off grid control aspects power quality issues etc [2]. Therefore, ensuring the secure and dependable operation of microgrids has become paramount. On top of that, the rapid expansion of global industrialization has led to an increased utilization of non-linear components, sensitive equipment, and relay protection devices. This trend has resulted in unwanted fluctuations in power signals. These deviations from standard values in voltage, current, or frequency are collectively known as Power Quality Disturbance Events (PQDEs). Common PQDEs include transients, harmonics, voltage sag/swell, unbalanced voltage/current, and interruptions. These disturbances can have serious consequences, including sympathetic tripping, protection and control device malfunctions, damage to sensitive electronic equipment, memory failures in monitoring systems, loss of productivity, and more. These repercussions affect industries, utilities, and consumers, with end users ultimately bearing the brunt of the consequences. This necessitates the development of a robust protection scheme capable of identifying and categorizing various types of Power Quality Disturbance Events. These events may occur due any intentional or unintentional operations in the microgrid which needed to be monitored as per IEEE PQ monitoring standard 1159-2009 [3].

To counter the aforementioned issue, a number of PQ detection techniques are reported in literatures that make use of the thresholds of system parameters [4], [5], [6], [7]. While these methods exhibit proficiency in detecting significant Power Quality (PQ) events, establishing appropriate detection thresholds involves balancing the rates of false alarms and accurate detections [8]. Furthermore, these techniques could exhibit susceptibility to factors like harmonics, sampling frequency, and various user-defined parameters. To overcome this particular issue, signal processing along with machine intelligence technologies are suggested by many authors [9] for automatic detection of PQDEs using the common principle displayed in Fig.1.

Various Signal Processing Techniques (SPTs) have been proposed for feature extraction in pattern recognition. These techniques utilize time-frequency transforms to differentiate disturbances. While the (Fast Fourier Transform) FFT suffers from spectral leakage and loss of time information [10], the fixed window length of (Short Time Fourier Transform) STFT makes it unsuitable for non-stationary transient signals [11]. To address this, Wavelet Transform (WT) methods have gained traction for analyzing such signals containing noise, fluctuations and sinusoidal components [12]. Further, out of discrete and continuous WTs, the Discrete Wavelet Transform (DWT) is preferred due to its adaptive window size and predefined filter design, making it suitable for preprocessing in classification tasks [13]. In Microgrid (MG) network, researchers have employed various intelligent classifiers for Power Quality Disturbances (PQDs) classification. Chakravorti et al. [14] used Reduced Kernel Ridge Regression (RKRR) combined with Variational Mode Decomposition (VMD) to detect islanding, faults, and PQ events in grid-connected MGs, achieving superior accuracy. Ranjbar et al. [15] employed Short-Time Fourier Transform (STFT) extraction with Decision Tree (DT) classification for accurate fault detection in both grid-connected and islanded MGs. Ray et al. [16] proposed Independent Component Analysis (ICA) for feature extraction combined with SVM for PQD classification, outperforming wavelet-based SVM. Nolasco et al. [17] used wavelet packet signal processing with fuzzy classifier, demonstrating effectiveness in detecting PQ factors like harmonics, power factor, and voltage variation in AC MGs under diverse conditions. In [18] a deep Convolutional Neural Network (CNN) approach is presented, known for noise immunity, accuracy, and speed in detecting single and multiple PQDs. Apart from that a number of single classifier-based PQ detection schemes are reported in literatures [19], [20], [21], and [22], those may suffer from under/overfitting, limited generalization ability, difficulty in handling higher dimension feature set etc. Ensemble classifiers [23], [24], [25] can be a solution, where a number of classifiers are trained to provide the result in voting approach. Therefore, the work emphasis on an ensemble machine learning technique (MLT) and chosen a base classifier called Kth Nearest Neighbour (KNN) due to its unmatched ability of handling unbalanced data, non-parametric nature, data adaptability, ease of feature and class scaling etc. Moreover, KNN can be ensembled by sub-spacing technique. Yungi Wang et al. [26] introduced a new feature extraction algorithm, normalized Renyi entropy, with KNN and SVM classifiers to predict PQ events in islanded MGs. In [9], various signal processing methods and classifiers were applied for detecting and classifying single and multiple PQDs in MGs where VMD with KNN showed higher classification accuracy.

The integration of PV systems into power grids can introduce several PQDs. However, the study focuses on the following key PQ concerns:

Voltage variations like sag and sell can be occurred due to unpredictable intermittent behaviour of solar output [27]. Certainly, a sudden shading of panels of the PV system can impose a drop in generation resulting in voltage sag. On the other hand, a swift elimination of shading can lead to swelling. A prominent imbalance of voltage can happen

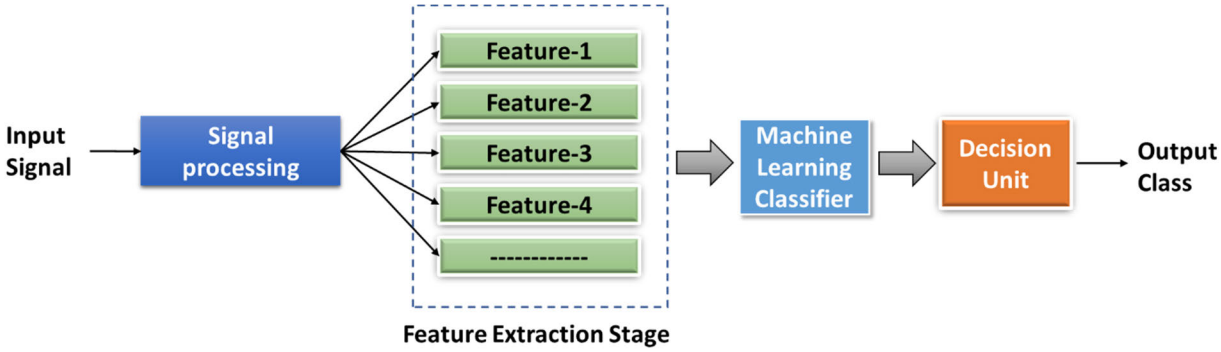

FIGURE 1. Power Quality Event Detection with signal processing and machine learner.

in case of unsymmetrical fault situations where one or two phases are found faulty. Apart from that, imbalance can also result due to highly penetrated single phase PV systems. The integration of PV in to grid is done through high frequency switching based power electronics inverters leading to harmonic distortions [28]. Along with that, the excess use of non-linear loads consumer end also injects notches like disturbances that can too introduce harmonics in the system.

Apart from that, transient behaviors can also be seen in PV integrated power systems. Connection and disconnection of PV from the grid and lightening hits can introduce momentary voltage spikes. Furthermore, capacitor switching is a frequent event in power system to facilitate voltage support, power factor correction etc., can introduces oscillatory transients. A noticeable variation in solar irradiance due to abrupt change in environmental condition such as large passing cloud can cause flicker disturbances which is troublesome to the end users [29].

Therefore, the research work deals with insightful feature extraction for performing effective PQDE classification and detection. This is possible if and only if the hidden component of the disturbance signal is uncovered through a powerful signal pre-processor. In addition to that, the performance of the classifier can be bolstered by effective ensemble applications to the existing classifiers. However, the three-phase quantity may or may not have any disturbance in all phases and might have in one or two phases. The study has taken all these problem statements in to account and following contributions are suggested:

- A novel Clarke's Transformation based signal reduction approach is adapted to create a unit signal which will facilitate the consideration of all three phases in to one signal.
- The signal preprocessor namely, Maximum Overlap Discrete Wavelet Transform (MODWT) is implemented to compute the multi-level components and the most efficient mother wavelet for PQDE detection is identified.
- A total of 16 features are obtained from 5-level detailed and an approximate component and fed to a proposed novel classifier called Subspace Weighted KNN, that shows significant outcomes while detecting the PQDEs.
- The detection time of the proposed MODWT-SWKNN classifier is obtained through OPAL-RT real time simulation by taking the mean of 500 disturbance observations.

The paper is structured as follows: Section II provides an overview of the PV integrated microgrid system, detailing specifications and power quality disturbance classes. Section III delves into signal pre-processing techniques. Section IV discusses the formation of the feature matrix. Section V explores the weighted subspace KNN classifier and its proposed optimization methods. Section VI presents the results and analysis of the study. Finally, the findings are summarized and concluded in Section VII.

II. MICROGRID SYSTEM DESCRIPTION

The considered microgrid is connected to 25 kV utility system through breaker-1(BR-1) as presented in Fig. 2. It is capable of operating both in on-grid mode and off-grid mode. The power requirement during on-grid mode of operation is fulfilled by the utility. Alternatively, off-grid mode is activated by opening the contacts of BR-2. During this off-grid period, the 400-kW solar plant will take the charge of power delivery. The solar plant consists of 4 number of 100 kW units cumulatively providing an output voltage of 500V DC through MPPT controlled DC/DC converter. This DC output voltage in converted to three phase AC through a PWM controlled voltage source converter and connected to grid followed by a LC-filter.

The specification and ratings of the microgrid elements and components are listed in Table-1. Moreover, the PQDs are simulated individually at the 25 kV BUS by actuating their respective breakers. The list of PQDs and the event specific categories, sources and indices are presented in Table-2.

III. SIGNAL PRE-PROCESSING

The initialization of the three-stage process of disturbance detection as shown in Figure 1. starts with signal pre-processing. The proposed work simplifies this stage as three substages as follows,

A. DATA COLLECTION

This is the first step of signal pre-processing where the voltage signal is kept on collected for a period 6 cycles with a

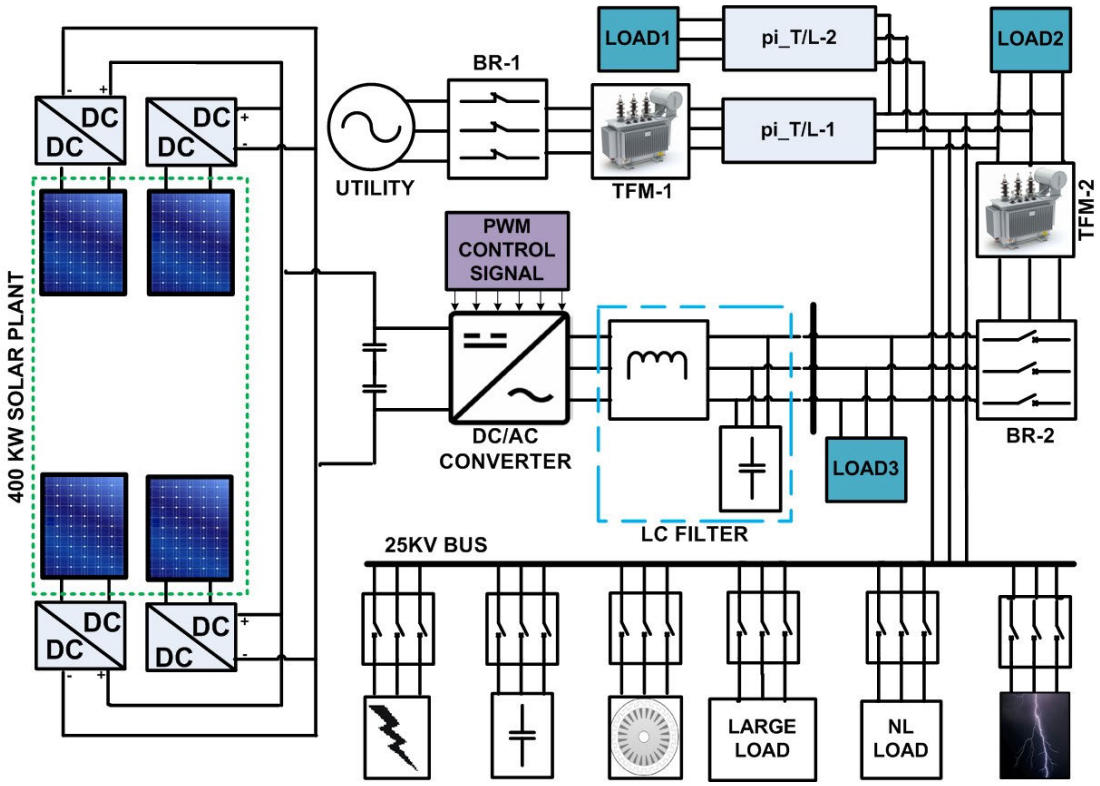

FIGURE 2. Circuit diagram of the solar enabled microgrid system.

TABLE 1. Microgrid component specification.

Microgrid components	Rating/specification
Utility	120KV, 50Hz, 2500MVA
TFM-1	120/25 KV, 50 MVA
pi_T/L-1	14 Km, 60 Hz
pi_T/L-2	8 Km, 60 Hz
LOAD1	30 MW, 2Mvar
LOAD2	2 MW, 2Mvar
Solar Plant	100KW*4 Units, 500V DC
Voltage source converter (VSC)	500KVA, 260 V
L-C Filter	45 μH, 40 KVAR
LOAD3	100 kW
TFM-2	0.26/25 KV, 450 KVA

TABLE 2. PQD events and categories.

POWER QUALITY CLASS	EVENT SOURCE	EVENT CATEGORY
PQC0	NORMAL	UNDISTURBED
PQC1	LG	SINGLE LINE SAG
PQC2	LL	DOUBLE LINE SAG
	LLG	
PQC3	SYMMETRICAL FAULT (LLLL & LLLG)	TRIPPLE LINE SAG
	TRANSFORMER ENERGIZATION	
	INDUCTION MOTOR STATING	
PQC4	LARGE LOAD SWITCHING OFF	VOLTAGE SWELL
PQC5	CAPACITOR SWITCHING	OSCILLATORY TRANSIENT
PQC6	LIGHTENING IMPULSE	IMPULSE TRANSIENT
PQC7	NON-LINEAR LOAD SWITCHING	VOLTAGE NOTCH (HARMONICS)
PQC8	ELECTRIC ARC FURNACE	FLICKER

gap of one cycle from the 25kV bus (Fig. 2). This continues process is carried out with 5kHz sampling frequency. The data vectors are stored in a database as rows in sequential manner. It is to be noted that the voltage data is converted to per unit before storage.

B. DATA REDUCTION

Various kinds of disturbances can initiate in a power network, affecting a single phase, either of the two phases, or all three phases. Consequently, it's crucial to account for all three phases during analysis. But such comprehensive analysis demands thrice memory space. A solution to this can be the conversion of three-phase component into a single-phase

component, leading to substantial reduction of processing time and minimal memory needs. One of such implementations is modal signal conversion [33]. But it is highly sensitive to unbalanced disturbances. Therefore, a novel approach is adapted in this work with the help of Clarke's Transformation. The basic form of Clarke's Transformation is as follows,

$$\begin{bmatrix} s_\alpha \\ s_\beta \\ s_0 \end{bmatrix} = \begin{bmatrix} \frac{2}{3} & -\frac{1}{3} & -\frac{1}{3} \\ 0 & \frac{1}{\sqrt{3}} & -\frac{1}{\sqrt{3}} \\ \frac{1}{3} & \frac{1}{3} & \frac{1}{3} \end{bmatrix} \times \begin{bmatrix} s_a \\ s_b \\ s_c \end{bmatrix} \tag{1}$$

The single signal is constructed by combining all three stationary reference frame components. Since sinusoids have an exceptional ability to generate other sinusoids with arithmetic operations, the new signal is obtained as,

$$s_{CTM} = (s_\alpha \times s_\beta) + s_o \tag{2}$$

The signal can be named as Clarke's Transformed Modal (CTM) Signal. It is to be noted that the signals must be converted to per-unit before making this conversion. A generic CTM of 6 cycle normal signal can be seen in Fig. 3.

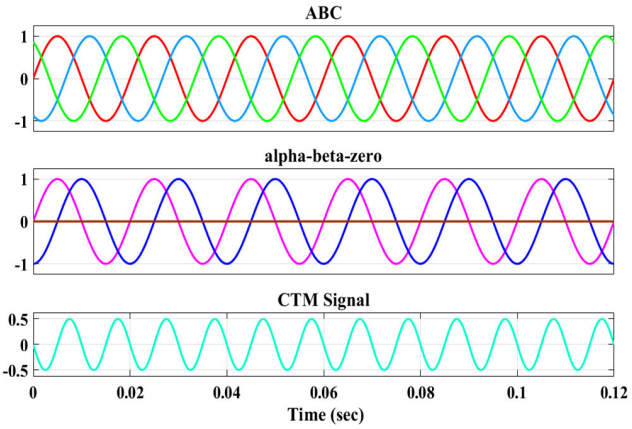

FIGURE 3. Clarke's transformed modal of a standard 3-phase sine wave.

C. DATA TRANSFORMATION (MAXIMUM OVERLAP DISCRETE WAVELET TRANSFORM)

Before getting in to MODWT, it is necessary to understand the basics of Wavelet Transform (WT). It proves to be a potent and efficient technique for analyzing swift transient signals that arise within power networks during faults and unusual incidents. By decomposing signals into various sub-components while localizing both the time and frequency domains, WT offers substantial utility. Typically, WT comes in two primary forms: Continuous Wavelet Transform (CWT) and Discrete Wavelet Transform (DWT). However, CWT is unsuitable for real-time applications due to its limited redundancy during signal reconstruction. In contrast, DWT addresses the CWT limitations by preserving the information of the input signal with least number of wavelet coefficients [32]. For any signal $u(t)$ DWT can be expressed as,

$$WT_D(i,k) = \frac{1}{\sqrt{a_0^i}} \sum_n u(n) * m\left(\frac{k - na_0^i}{a_0^i}\right) \tag{3}$$

Here, a_0^i: scaling factor, na_0^i: Translational Factor, $m(\cdot)$: mother wavelet, i, j: non-negative integer values, k: sample number in input signal.

DWT performs a successive decomposition-reconstruction of the disturbance signal using multi-resolution analysis. In this process two types of components are obtained namely approximate component (APC) and detailed component (DTC) in each level. In the first level, the APC-1 is obtained from a low pass filter (F_{LP}) whereas the DTC-1 are obtained from a high pass filter (F_{HP}). Further, APC-1 is decomposed on a similar fashion to obtain APC-2 and DTC-2 respectively and it continues till reaching number of levels demanded. It is to be noted that, after every decomposition stage the sampling frequency of the signal is made half. A glimpse of the process can be seen on Fig. 4 which can be mathematically represented as,

$$Input\ Signal, I(k) = \sum_{i=1}^{n} DTC_i + APC_n \tag{4}$$

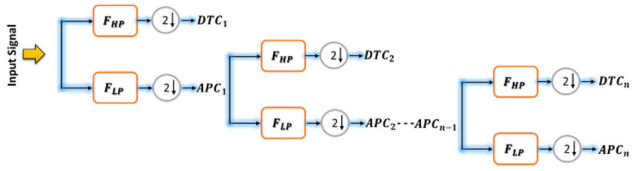

FIGURE 4. n-level DWT.

In this study a more effective version of DWT is implemented called Maximum Overlap Discrete Wavelet Transform (MODWT) that employs filters similar to DWT, but with the overlap between adjacent sub-bands. It helps to reduce the boundary effects caused by filtering and down-sampling. It further reduces the edge effects and allows for a more accurate representation of the signal at different scales. Moreover, MODWT can act on both stationary and non-stationary components. The overlapping sub-bands can better capture the transient behaviour of signals [31]. Due to such characteristics, it can be extremely useful for analyzing nonlinearity, transient and noise component present in power signals.

IV. FEATURE EXTRACTION

The second stage of the three-stage process of disturbance detection as shown in Fig. 1 is feature extraction. When designing features for a machine learning classifier, it's important to choose features that are relevant, informative, and representative of the underlying patterns in the data. The specific features one MLC require will depend on the nature of the problem and the type of data. Therefore, the choice of features (also known as feature engineering) is a critical step in building effective machine learning classifiers.

Since, the chosen signal processor MODWT has inherent property of preserving energy [31], the first feature is chosen

to be a unique component called detail to approximate component energy ratio (DTAER). This can be defined as,

$$DTAER_{DTC_j} = \frac{e_{DTCj}}{e_{APC}} = \frac{\sum_{k=1}^{K} DTC_j^2(k)}{\sum_{k=1}^{K} APC^2(k)} \quad (5)$$

Secondly, the high frequency detailed component generally has a greater number of zero crossings to that of the approximate component. A ratio of these two can provide hidden insights of the presence of high frequency components in the signal. Therefore, the next feature called detail to approximate component zero crossing ratio (DTAZCR) can be,

$$DTAZCR_{DTC_j} = \frac{ZC_{DTCj}}{ZC_{APC}} \quad (6)$$

In general, a pure sinusoid is ideally having zero mean. But the data reduction technique adapted in this study are generating CTM signals not uniform around the axis in most cases if any disturbance exists. The same phenomenon will also propagate to MODWT multilevel decomposition of any signal. Therefore, the simplest feature named mean of a signal can be taken for all detailed and one approximate component.

$$MEAN_{MODWT_j} = \frac{\sum_{k=1}^{K} s(k)}{K} \quad (7)$$

V. PROPOSED CLASSIFIER

KNN (K-Nearest Neighbour) is a non-parametric instance-based learning method that provides solutions for problems with unknown distributions, particularly in non-nominal cases [37]. In instance-based learning, a distance metric function is employed to compare the characteristics of each new instance with existing ones. The nearest instance is then used to assign a class to the new instance. If a greater number of nearest Neighbour are considered, the class assigned to the new instance is determined by the majority class among the nearest k Neighbour [37]. One of the numerous factors impacting the performance of the KNN algorithm is the selection of the hyperparameter k. If k is set to a small value, the algorithm becomes more sensitive to outliers. Conversely, if k is chosen to be too large, the neighbourhood might encompass an excessive number of points from different classes. Another concern is the strategy for aggregating class labels. The most straightforward approach is to rely on the majority vote, but this can be problematic when the nearest Neighbour exhibit significant variations in distance, and the closest Neighbour more consistently represent the object's class. To understand this an example is taken in Fig. 5.

Here 4 different classes (C1, C2, C3, C4) with a single feature are presented. If the unknown data is required to be determined through KNN classifier, it will predict different classes randomly in every trial. But to naked eyes it is clearly seems to be nearer to C3. To overcome this drawback, weighted KNN (WKNN) can be utilized which is an extension of the traditional KNN algorithm. In the standard KNN algorithm, each of the k nearest Neighbour

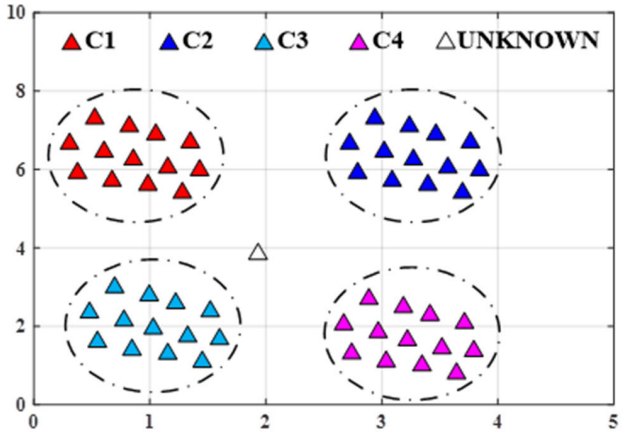

FIGURE 5. A single feature representation for 4 classes.

contributes equally to the classification decision. However, in the WKNN classifier, the influence of each Neighbour on the classification is weighted based on certain criteria often called a kennel function. Typically, the weight is inversely proportional to the distance, meaning that closer Neighbour have a greater influence on the classification decision, while more distant Neighbour have a reduced influence.

Moreover, to tackle the challenges occurred due to high dimensionality of the feature space, the random subs-pacing technique is also utilized along with WKNN. Sub-spacing introduces a randomization factor by considering only a subset of the available features to create a sub-classifier. Further an ensemble of sub classifiers together makes the prediction with a voting approach. This improves the generalization ability, provides robustness against irrelevant features and the ensemble classifier as a whole becomes noise tolerant.

If there are s subspaces such that,

$$SS = [S_1, S_2, - - -, S_s] \quad (8)$$

And there are f features such that,

$$F = [f_1, f_2, - - -, f_f] \quad (9)$$

Further, $\grave{F}$ is any random subset of F such that $\{\acute{F}_1, \acute{F}_2, - - -, \acute{F}_s\}$ and if the dataset is denoted by D and $\acute{D}$ is a random subset of D such that $\{\acute{D}_1, \acute{D}_2, - - -, \acute{D}_s\}$ then each subspace S_j will going to be trained with only $\acute{F}_j$ features and $\acute{D}_j$ sub-dataset.

Furthermore, in each subspace S_j WKNN is performed as follows,

$$P(T = t \mid F = X_o) = \frac{1}{k} \sum_{(X_i, t_i) \in \acute{D}_j} w_i \times I(t_i = t) \quad (10)$$

Here, P denotes the conditional probability of each class. X_o is the observation feature column matrix. w_i is the weight. $I(\cdot)$ is a Boolean operator that turns 1 when the given observation (X_i, t_i) belongs to the class t else 0.

VI. RESULT AND DISCUSSION

The performance evaluation of the proposed MODWT-SWKNN based PQ Detection system for gid connected PV is discussed in this section. Initially, the model shown in Fig. 2 is designed and simulated in MATLAB Simulink environment. The PQ event classes (PQC-0 to PQC-8) are intentionally simulated at 0.1 sec. A 6-cycle data is getting captured with a sampling frequency of 5kHz (100 data samples/cycle) i.e., 600 data samples at 100 sample gaps between each sample collection instant. At every sample collection instant, all the three-phase data are arithmetically combined to form the CMT signal. This resulting signal is further processed through MODWT multistep decomposition process to obtain 5 detailed and one approximate component. Further 16 features are obtained from the decomposed signals and fed to the SWKNN classifier to obtain the class of disturbance. A flow diagram describing the work flow mentioned above is shown Fig. 6. The choice of mother wavelet, value of K in WKNN and the number of subspace variables are discussed in the later sections.

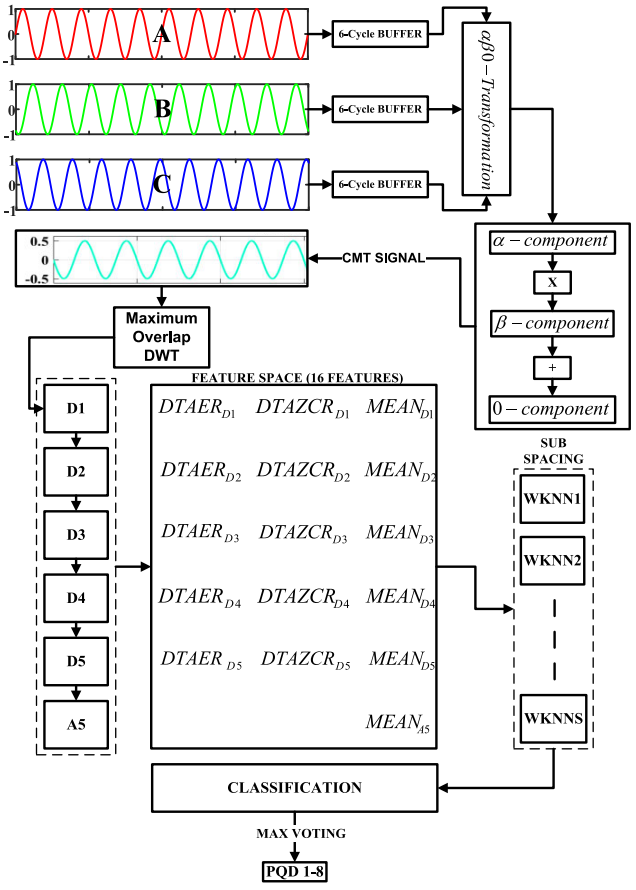

FIGURE 6. Flow diagram of the proposed work.

A. WAVE FORM ASSESSMENT

Fig. 7 displays a single line sag event, which is intentionally created in the test system by simulating a LG-Fault. The initial disturbances at simulation starting are presented with

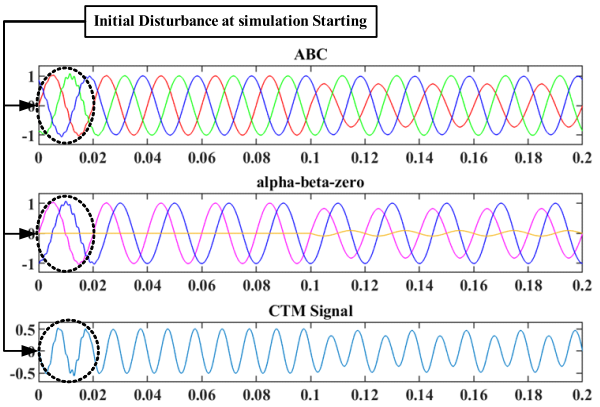

FIGURE 7. One line sag.

dotted elliptical circles which are occurred just before the synchronization and control algorithms takes their control.

The fault has been initiated at 0.1 sec to ensure the intentional disturbance should not interfere with the initial disturbances. The subsequent disturbance event plots (Fig. 8) are therefore only shown for 6 cycles i.e., 3 before and other 3 after the initiation of disturbance events. It can be clearly observed from Fig. 8 the CTM signals of different PQ events are distinctive with respect to each other. It can be seen that; the unbalanced disturbances display good presence in zero sequence component where the balance disturbances have null or negligible presence. This particular fact is used as an advantage in this study and a good arithmetic mix of Clark's Transformed signals is obtained to analyses the class of disturbance.

B. DATASET FORMATION

Dataset formation simply means to create a tabular data containing the features in columns along with the respective class of event. The rows of the dataset represent different occurrences of the events. Similarly, 5400*16 feature set and a 5400*1 target set collectively forms the PQC dataset of this study. Here 600 observations from each of the PQ disturbance class have been created by processing the three-phase voltage data collected at PCC of the studied system. This is termed as Ideal Dataset (IDS). Moreover, on a technical aspect, the fault data are collected with different fault resistances. Swell signals are generated by suddenly removing different magnitude of larger loads. Oscillatory Transients are generated with varying capacitor bank switching. Further impulse transients are created by lightening block with varying impulse amplitude. Similarly harmonic signals are generated by non-linear load switching with varying the passive components. Lastly flicker is initiated by Electric Arc Furnace switching.

However, in pure simulation environment there is no external impact on the power system however in practical system the lines undergo electromagnetic interference. In this regards, Signal-to-noise ratio (SNR) comes in to picture which is a measure of how much signal power is present in an electrical signal compared to how much noise

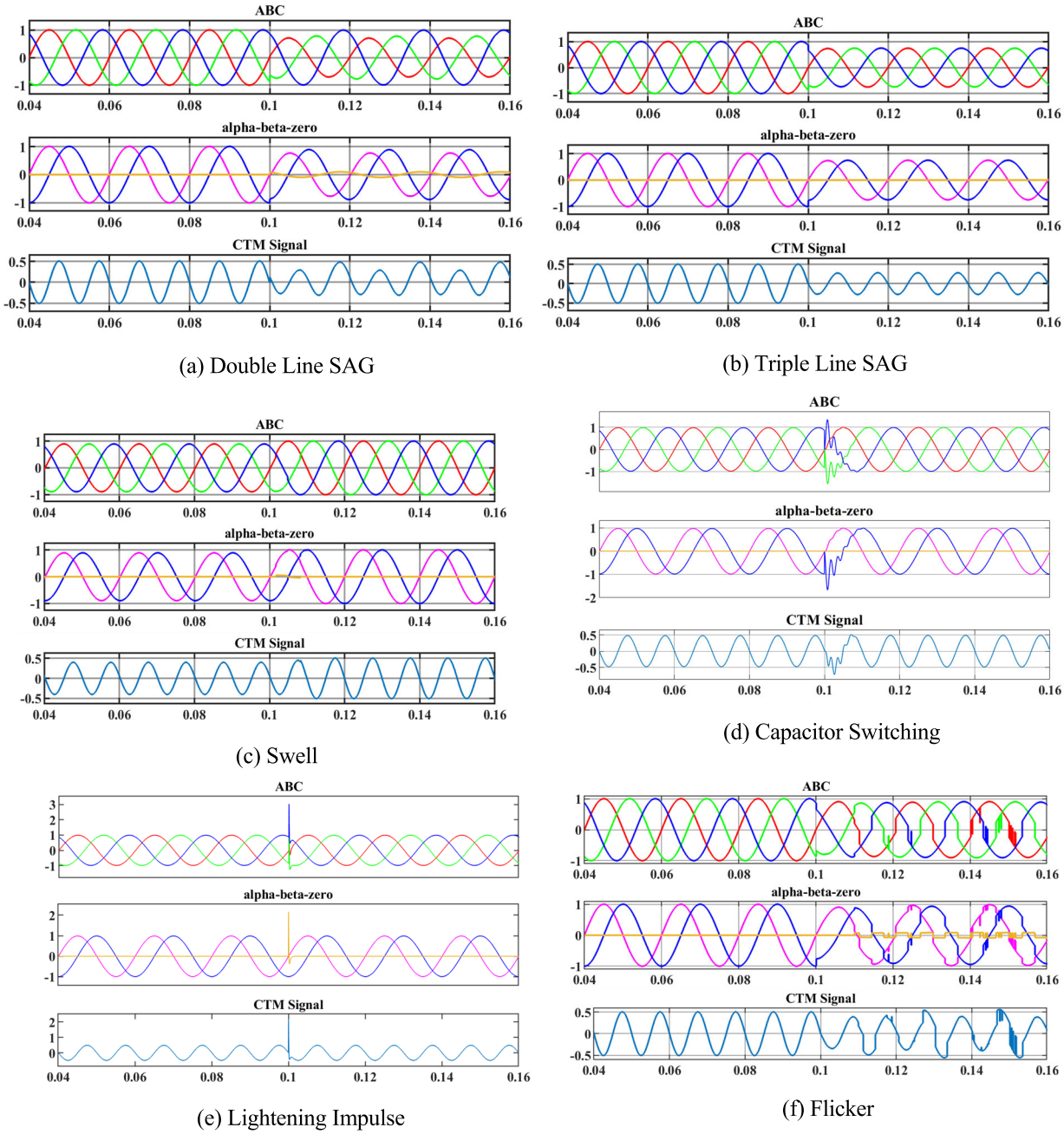

FIGURE 8. Other PQ disturbances.

power is present. It is often expressed as a decibel value. Mathematically,

$$SNR\,(in\ dB) = 10log\frac{S_p}{N_p} \tag{11}$$

where, S_p is the power of the signal and N_p is the power of the noise.

Therefore, to realize the real-world scenario another dataset is formed by adding white gaussian noise to the existing dataset such that 20dB, 30dB and 40dB noise is added to 200 feature set of each event. This will create another feature matrix termed as Noisy Dataset (NDS). It has exactly the same dimension that of IDS. Both of these datasets have the same representation as shown in Table-3.

C. OPTIMUM SWKNN PARAMETER SELECTION

Once the dataset is prepared, the next step is to perform the classification task. The study leverages the unique advantages of the KNN classifier, such as its seamless adaptation to new data, does not require explicit model building, lazy learning characteristics, and real-time predictability. However, KNN also has certain limitations, including sensitivity to outliers,

TABLE 3. Dataset Format with 16 features and 0 to 8 PQCs.

SL	F1	F2		F16	CLASS
1			-----		PQC0
2			-----		PQC0
3			-----		PQC0
		-----			-----
600			-----		PQC0
	-----		-----	-----	PQC1 to PQC 7

4801			-----		PQC8
4802			-----		PQC8
4803			-----		PQC8
		-----			-----
5400			-----		PQC8

reduced performance with large datasets, and a high dependency on the choice of 'k' value. To address the limitations of the traditional KNN classifier, this study introduces two enhancements: 'weighting' and 'sub-spacing'.

1) WEIGHTED KNN

This method is less sensitive to outliers because it assigns more weight to nearby points and less to distant ones, which helps decode underlying data patterns and improves classification accuracy. Additionally, it handles imbalanced, complex, and non-linear data distributions more effectively.

2) SUB-SPACING

This involves using a group of classifiers, each trained on a subset of the data with fewer feature variables. This approach enhances generalization, reduces bias, and provides robustness against irrelevant and noisy data. By combining the predictions of multiple models, ensemble methods improve decision-making in KNN, resulting in more accurate and robust classification, particularly in the presence of outliers or complex data patterns.

As a result, the proposed subspace-weighted KNN establishes a refined and smoother decision boundary, leading to more accurate decision-making when the classifier encounters unknown data. Further it requires to obtain three major hyper-parameters such as,

- Number of Subspaces
- Number of Features in Each Subspace
- Number of Neighbours

First of all, the number of classes taken in the study are 9, therefore one cannot go below 9 neighbours which may lead to undesired outcomes. But the nominal rule for the selection of 'k' in traditional KNN is square root of the available dataset i.e., $\sqrt{5400} = 73.48$. Therefore, the number of subspaces can be set at $73.48/9 = 8.16 \approx 8$ such that there will be 9 neighbours in each subspace. Now the decision variables (features) in each subspace should be within 2 to 15 as the total number of available variables are 16. If it is set to be very low then that will affect the detection ability where if set to high will increase computational burden. Therefore, a mathematical study is done between the detection accuracy and computational time to evaluate the number of decision variable. It is to be noted that, the mother wavelet is set to 'sym4' which is default for MODWT. Moreover, each observation is 10-fold cross validated and the average accuracy and computation time are presented in Table-4.

TABLE 4. Accuracy and computation time for different decision variable count in subspaces.

DECISION VARIABLE COUNT	ACCURACY	COMPUTATION TIME (IN MS)
2	27.52%	15.4
3	36.04%	26.7
4	43.56%	34.9
5	51.75%	44.5
6	59.27%	52.7
7	72.5%	68.3
8	87.1%	81.9
9	87.33%	99.7
10	87.47%	123.5
11	87.53%	157.2
12	87.64%	168.2
13	87.83%	183.7
14	87.91%	201.6
15	87.97%	219.4

It can be observed that, the detection accuracy remains steady near 87% when 8 or more variables are taken in a subspace. But the overall computation time drastically increasing with each surplus variable without significant improvement in detection accuracy. Therefore, the random variable per subspace is set to 8 so as to maintain an optimum computation time without compromising the accuracy. The obtained parameters for SWKNN are displayed in Table-5.

TABLE 5. SWKNN parameter values.

NO. OF SUBSPACES	NEIGHBOUR PER SUBSPACE	FEATURE PER SUBSPACE
8	9	8

D. MODWT MOTHER WAVELET SELECTION

Further, the selection of best mother wavelet for the data preprocessing stage could be a crucial factor which will hugely affect the detection accuracy. To identify the same, all kinds of orthogonal wavelet are rigorously tested with SWKNN classifier with all possible wavelet combinations as shown in Table-6. It can be clearly observed from Table-6 that the Discrete Meyer Wavelet ('dmay') shows the highest accuracy of detection amongst all other orthogonal wavelet variants. Hence 'dmay' is chosen as the mother wavelet in this study. It is to be noted that the parameter obtained for SWKNN as of Table-5 are used in this testing.

E. PERFORMANCE EVALUATION

The optimum MLC parameters along with the best mother wavelet for MODWT are determined in the previous

TABLE 6. Optimum mother wavelet selection.

MOTHER WAVELETS FAMILY	VARIANTS OF WAVELET	OPTIMUM WAVELET	OPTIMUM ACCURACY
HAAR	'DB1'	'DB1'	90.4%
DAUBECHIES	'DB2' TO 'DB45'	'DB15'	93.06%
SYMLETS	'SYM2' TO 'SYM45'	'SYM7'	88.1%
COIFLETS	'COIF2' TO 'COIF5'	'COIF3'	95.31%
DMEYER	'DMEY'	'DMEY'	99.74%
FEJER-KOROVKIN	'FK4', 'FK6', 'FK8', 'FK14', 'FK18', 'FK22'	'FK6'	94.31%

True Class \ Predicted Class	PQC0	PQC1	PQC2	PQC3	PQC4	PQC5	PQC6	PQC7	PQC8	Class Accuracy
PQC0	600	0	0	0	0	0	0	0	0	100%
PQC1	0	600	0	0	0	0	0	0	0	100%
PQC2	0	0	600	0	0	0	0	0	0	100%
PQC3	0	0	0	594	6	0	0	0	0	99%
PQC4	0	0	0	5	595	0	0	0	0	99.16%
PQC5	0	0	0	0	0	598	0	2	0	99.66%
PQC6	0	0	0	0	0	0	600	0	0	100%
PQC7	0	0	0	0	0	1	0	599	0	99.83%
PQC8	0	0	0	0	0	0	0	0	600	100%
									Overall Accuracy	99.74%

FIGURE 9. Confusion Matrix of Ideal Dataset (IDS).

True Class \ Predicted Class	PQC0	PQC1	PQC2	PQC3	PQC4	PQC5	PQC6	PQC7	PQC8	Class Accuracy
PQC0	594	0	0	0	0	0	0	6	0	99%
PQC1	0	593	7	0	0	0	0	0	0	98.8%
PQC2	0	6	594	0	0	0	0	0	0	99%
PQC3	0	0	0	593	7	0	0	0	0	98.8%
PQC4	0	0	0	12	588	0	0	0	0	98%
PQC5	0	0	0	0	0	575	0	25	0	95.8%
PQC6	0	0	0	0	0	0	600	0	0	100%
PQC7	0	0	0	0	0	22	0	572	6	95.33%
PQC8	0	0	0	0	0	0	0	9	591	98.5%
									Overall Accuracy	98.14%

FIGURE 10. Confusion Matrix of Noisy Dataset (NDS).

subsection. On account of those the performance of MODWT-SWKNN power quality detection scheme is evaluated in this subsection. Here, three other performance indices (PIs) are evaluated along with detection accuracy as of (12), (13), (14). But the perquisites for calculating the PIs is the confusing matrix. Therefore, the confusion matrices of both IDS and NDS datasets are presented in Figure 9 and Figure 10. It can be seen that the overall accuracy of ideal dataset is found to be 99.74% whereas for noisy dataset it is 98.14%. It can also be observed that the PQC6 i.e., the impulse transient data are detected with 100% accuracy both in ideal and noisy scenarios. Additionally, a 20dB confusion matrix is also presented in Figure 11, so as to take a glimpse of the classifier performance under dense noise. It seems that, the performance is still maintained over 97% even under the highly noisy conditions.

The performance indices are as follows,

$$Precison, P_X = \frac{C_X}{C_X + \hat{C}_x} \tag{12}$$

$$Recall, R_X = \frac{C_X}{C_X + \overline{C}_X} \tag{13}$$

$$F1Score, F1_X = \frac{2 * (P_X * R_X)}{P_X + R_X} \tag{14}$$

True Class \ Predicted Class	PQC0	PQC1	PQC2	PQC3	PQC4	PQC5	PQC6	PQC7	PQC8	Class Accuracy
PQC0	197	0	0	0	0	0	0	3	0	98.5%
PQC1	0	195	5	0	0	0	0	0	0	97.5%
PQC2	0	3	197	0	0	0	0	0	0	98.5%
PQC3	0	0	0	196	4	0	0	0	0	98%
PQC4	0	0	0	7	193	0	0	0	0	96.5%
PQC5	0	0	0	0	0	189	0	11	0	94.5%
PQC6	0	0	0	0	0	0	200	0	0	100%
PQC7	0	0	0	0	0	9	0	188	3	94%
PQC8	0	0	0	0	0	0	0	4	196	98%
									Overall Accuracy	97.28%

FIGURE 11. Confusion Matrix under 20dB noise.

where, C_X is number of events truly detected as class -X

$\overline{C}_X$ is number of events truly belongs to class -X but detected as any other class

$\widehat{C_x}$ is number of events do not belongs to class -X but detected as class -X

The bar chart representations have been made to showcase different PIs valuation for every PQC in Fig. 12 considering both ideal and noisy datasets. Here Fig. 12(a) displays the outcome for IDS whereas Fig. 12(b) for NDS. While all the

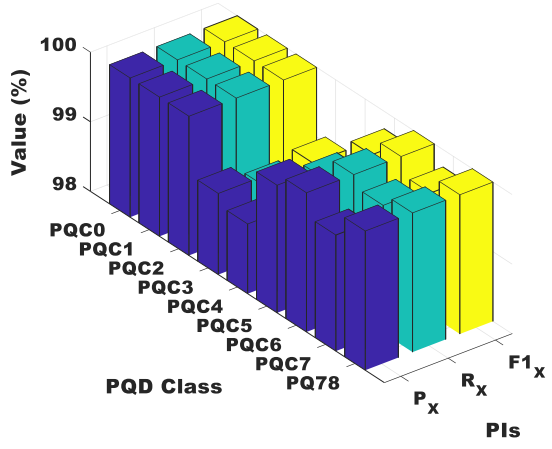

(a)Bar Diagram IDS

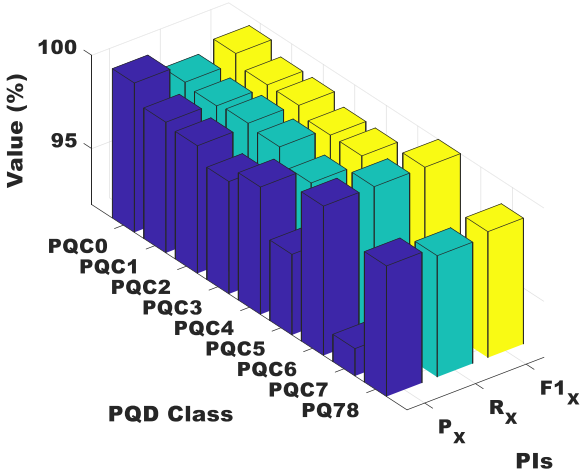

(b)Bar Diagram NDS

FIGURE 12. Bar chart of performance indices.

PIs of IDS are well above 98%, the PIs of NDS for PQC7 are as low as 93.46%, 95.33% and 94.38% (precision, recall, F1-score) respectively. But the overall detection accuracy under noisy data condition is still sitting at 98.14%. Hence, the MODWT-SWKNN classifier can be a good choice to be implemented in real world PV based microgrid scenarios.

F. PERFORMANCE IN LARGE POWER SYSTEM

The performance of the proposed detection strategy is now getting verified in a PV integrated large power system. Such a system can be seen in Fig.13 where an IEEE 13 bus system is modified to study the impact of PV penetration [40]. The PV system is of rating 1 MW and integrated at bus 680 via T_3 transformer and two stage power electronics converters.

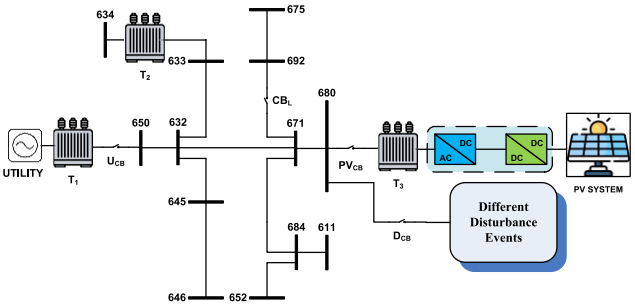

FIGURE 13. PV integrated IEEE 13-Bus modified system.

Exactly same number of i.e., 9, PQ events are also tested here as if in the PV-tied power system shown in Fig. 2. The same 16 features are also extracted by simulating different disturbance events intentionally in MATLAB environment to generate a new dataset that consist of both ideal and noisy data with 1200 events per class. The detection accuracy of the proposed classifier with the new large power system dataset (10800*16). Then the proposed SWKNN classifier is undergone training and testing procedure. To evaluate its accuracy the full confusion matrix is presented in Fig.14. It is observed that each of the disturbance events are displaying more than 99% accuracy individually except PQC7. The overall accuracy of detection is also found to be 99.28% displaying the splendid classification capability of the classifier. After verifying the result obtained from both test system, the performance remains consistent in both small and large power systems.

		Predicted Class									Class
		PQC0	PQC1	PQC2	PQC3	PQC4	PQC5	PQC6	PQC7	PQC8	Accuracy
True Class	PQC0	1190	0	0	0	0	0	0	10	0	99.16%
	PQC1	0	1194	6	0	0	0	0	0	0	99.5%
	PQC2	0	8	1192	0	0	0	0	0	0	99.33%
	PQC3	0	0	0	1191	9	0	0	0	0	99.25%
	PQC4	0	0	0	5	1195	0	0	0	0	99.58%
	PQC5	0	0	0	0	0	1193	0	7	0	99.42%
	PQC6	0	0	0	0	1	0	1199	0	0	99.91%
	PQC7	0	0	0	0	0	10	0	1181	9	98.41%
	PQC8	0	0	0	0	0	0	0	12	1188	99%
										Overall Accuracy	99.28%

FIGURE 14. Overall confusion matrix of large power system dataset.

G. REAL-TIME VALIDATION

The results presented in the previous subsections are found through the model designed in MATLAB Simulink as well as MATLAB script executions. But the outcomes are not enough to assure whether the proposed MODWT-SWKNN PQ Detection scheme will perform in practical grid scenarios or not. To resolve this concern, the PQ detection scheme is tested in OPAL-RT real time simulation setup as shown in Fig. 15(a). First, the Simulink model is designed in the Host PC and the respective C-codes are built in RT-LAB software platform. Further it is loaded to OPAL-RT 4510 setup and the real-time simulation is executed and results are opted in YOKOGAWA multi signal oscilloscope (MSO) as shown in Fig. 15(b). The detection is identified by an Event Index (EI) varies from 0.5 to 4 as per Table-2. It can be observed that, there is a detection delay from the point of occurrence

(a)Real-Time Setup with MSO and HOST PC

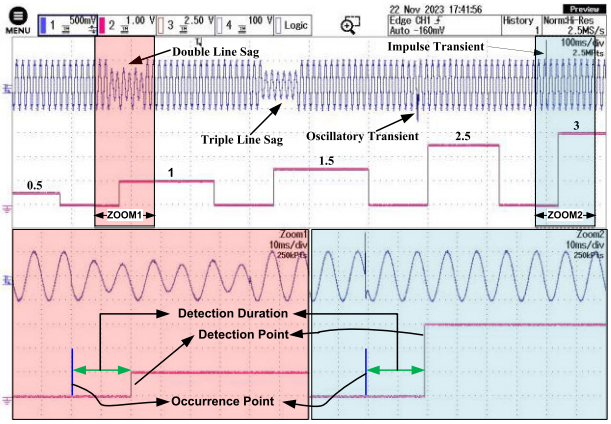

(b)Disturbance CTM Signal and detected event indices

FIGURE 15. Real time validation.

to point of detraction. It is obvious because, the proposed detection scheme itself taking a 6-cycle snapshot with a gap of one cycle, thereby introducing a fixed delay of one cycle or 0.02 secs. This phenomenon reduces the computational complexity significantly and also provide a CPU cool off period in between successive snapshots.

However, there are some variable delays observed along with fixed delay which differs from event to event. To counter this discrepancy, a set of 500 observation are saved during real time simulation and the average of sample difference between point of occurrence are detection are evaluated to calculate the detection time. Such an obtaining can be seen in Fig. 16. Finally, the mean detection time is calculated from the average detection difference of 142.3881samples with 5Hz frequency as 0.0285sec (142.3881/5000).

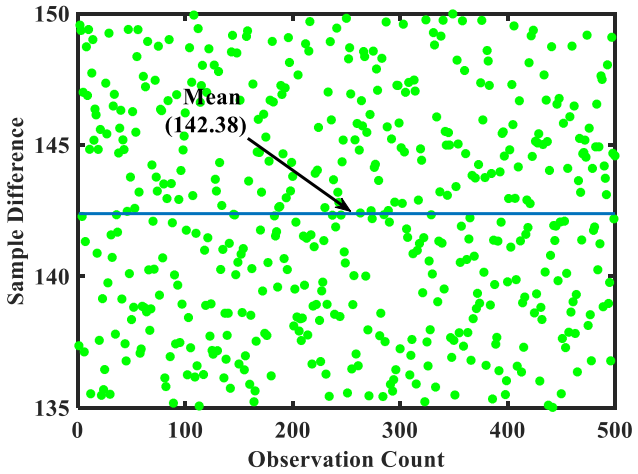

FIGURE 16. Average detection time calculation with 500 observations.

H. COMPARATIVE STUDY

A comparative study involving the performance of various recently published PQ detection scheme in PV integrated system are presented in Table-7. The performance of these methods in terms of detection accuracy are observed both under ideal and noisy conditions with 3 SNR levels of 20dB, 30dB and 40dB respectively. Although [16], [34], [35], [36], [39] have claimed to possess 100% ability of detection in ideal condition but do not provide any information regarding the performance under noise. Similarly, [37] and [38] have tested under moderate noise but haven't goes through the dense noise of 20dB. While [33] have been tested with all 3 noise levels but its performance suffers under heavy noise and accuracy goes down to 94.7%. Since in practical grid scenarios, the current carrying conductors often experience electromagnetic interference which is highly important to be considered while designing a detection system. Therefore, the study tested the performance both under ideal and noisy conditions. Moreover, limited studies have focused upon the detection time [16], [40]. Although studies in [41] and [42] have tested 15, 28 events respectively and obtained good performance on accuracy but haven't gone through the detection time evaluation. However, the study performed real-time detection of the proposed scheme through OPAL-RT 4510 setup and the detection time is calculated as explained in previous sub-subsection. Although studies made in [16] and [40] obtained the detection time, but lacking precise observations to made during the calculation of it. However, one should take in to account the factors like cycles to capture, signal propagation delay, detection algorithm process delays etc. These factors are already included in the applied real-time setup, hence an accurate detection time of 0.0285 secs is obtained in this study.

I. CRITICAL DISCUSSION

In this study, the grid-connected PV model is designed and simulated in the MATLAB 2018a Simulink environment. Once the model is ready, PQ disturbances are intentionally introduced at the 25kV bus at a specific time, say 0.1 seconds, as per Table-2. Then, a 6-cycle voltage data is stored, with 3 cycles before and after the disturbance occurrence to prepare the dataset. The main challenge in the data extraction stage is to get replication of real scenario data to make the classifier learn the inherent characteristics of the events. Therefore, each disturbance event data is collected with utmost care by following sustainable variations in system parameters or scenarios to maintain proper data diversity with minimal redundancy.

As the study deals with a three-phase system, the authors propose a novel three-to-one signal conversion technique using Clarke's Transformation, named Clarke Transformed Modal (CTM). This approach handles the three-phase signal as a whole, avoiding the need to analyze each phase individually. In the process of signal decomposition, it is important the capture the intrinsic components of the power signal along with intermediate transients. Therefore, the MODWT signal preprocessor is used to retrieve the inherent constituents of the CTM signal. MODWT eliminates boundary effect concerns, can act on both stationary and non-stationary signals, and the overlap between adjacent bands helps in capturing transients. The three-to-one signal conversion approach reduces the preprocessing overhead to one-third of the resource utilization.

Moreover, the study leverages the unmatched advantages of KNN classifiers. Since KNN is distance-based, retraining is not required when new data is added to the training set. However, due to challenges like the curse of dimensionality, outlier sensitivity, and memory intensiveness, the authors propose SWKNN as a possible solution. The MODWT-SWKNN classifier is tested under different levels of noise and found to be noise-robust. The next challenge is its real-time implementation in actual grid scenarios, which will involve measurement sensors at critical points, analog-to-digital converters, data acquisition systems, and microcontroller-based parallel processing units. However, prior to implementation, real-time validation is required. This is performed in the

TABLE 7. Comparative analysis with previously reported PQD detection schemes in PV equipped microgrids.

SL. NO.	METHODS	PQC	MODEL PERFORMANCE (IN ACCURACY %)				TIME OF DETECTION (IN SECS)
			IDEAL ACCURACY	NOISY ACCURACY (SNR IN DB)			
				20	30	40	
1	[16]	6	99.5	-	-	-	0.07
2	[33]	5	-	94.7	97.2	99.75	-
3	[34]	16	98	-	-	-	-
4	[35]	10	100	-	-	-	-
5	[36]	10	97	-	-	-	-
6	[37]	9	99.59	-	99.5	99.29	-
7	[38]	14	99.82	-	99.29	-	-
8	[39]	7	100	-	-	-	-
9	[40]	16	100	97.54	99.81	99.96	0.184
10	[41]	15	-	-	99.06	99.18	-
11	[42]	28	-	97.65	99.35	99.40	-
12	PROPOSED	9	99.74	97.28	97.94	99.22	0.0285

OPAL-RT setup, where the designed MATLAB test system is implemented in an FPGA unit.

VII. CONCLUSION

PV penetration to the existing power grid is exponentially increasing both in domestic and industrial sectors, impacting operations and quality of power. Thus, PQ event identification is essential in PV integrated power systems from protection, stability, reliability, and PQ management standpoints. Effective detection and mitigation strategies are crucial for maintaining high power quality standards. With the aforementioned context, the study primarily targets the detection of 9 distinct power quality events in a grid-tied photovoltaic system. It introduces a novel signal reduction technique named Clark Transformed Modal to convert the three-phase point of common coupling (PCC) voltage into a single modal signal. This transformation reduces memory usage and computational complexity during signal processing. Subsequently, 16 intrinsic features (such as DTAER, DTAZCR, and MEAN) are extracted from 6-cycle windowed CTM signals using a five-level Maximum Overlap Discrete Wavelet Transform (MODWT) decomposition. The resulting dataset, comprising 10800 entries with 16 features each, includes both ideal and noisy data for all 9 power quality events, with 1200 disturbances per event. An enhanced version of the K-nearest neighbor (KNN) classifier, termed Subspace Weighted KNN (SWKNN), is proposed to efficiently manage high-dimensional data. The study finds that dividing the data into 8 subspaces, each containing 9 neighbors and 8 features, achieves the highest detection accuracy of 99.74% using the Discrete Meyer mother wavelet on the ideal dataset. The classifier also proves robust to noise, achieving accuracies of 99.22%, 97.94%, and 97.28% under signal-to-noise ratios (SNR) of 40dB, 30dB, and 20dB, respectively. Additionally, the mean detection time for the proposed MODWT-SWKNN classifier is determined to be 0.0285 seconds, based on the average detection time of 500 random events in the OPAL-RT 4510 real-time simulation environment. This work is also extended to a large PV integrated IEEE 13-Bus modified power system and evidenced promising detection accuracy of 99.28%. The study compares its findings with several previous works focused on power quality detection in grid-tied PV systems and concludes that the proposed method offers superior detection accuracy and speed, making it suitable for real-world grid applications.

In the future research, a broader range disturbance including simple, complex and mixed power quality events can be investigated to improve the versatility of the MODWT-SWKNN classifier. Actual grid integration along with and self-tuning mechanisms can be developed to enable the detection system for adaptive learning that can learn from unseen real-time data. Furthermore, protection and security concerns can be addressed to ensure robustness against external challenges.

REFERENCES

[1] E. Mulenga, M. H. J. Bollen, and N. Etherden, "A review of hosting capacity quantification methods for photovoltaics in low-voltage distribution grids," *Int. J. Electr. Power Energy Syst.*, vol. 115, Feb. 2020, Art. no. 105445.

[2] A. Sharma, M. Kolhe, A. Kontou, D. Lagos, and P. Kotsampopoulos, "Solar photovoltaic-based microgrid hosting capacity evaluation in electrical energy distribution network with voltage quality analysis," *Social Netw. Appl. Sci.*, vol. 3, no. 5, pp. 1–22, May 2021.

[3] *IEEE Recommended Practice for Monitoring Electric Power Quality*, Standard IEEE Std 1159-2019, 1159, pp. 1–98.

[4] A. Furlani Bastos, W. Freitas, G. Todeschini, and S. Santoso, "Detection of inconspicuous power quality disturbances through step changes in rms voltage profile," *IET Gener., Transmiss. Distrib.*, vol. 13, no. 11, pp. 2226–2235, Jun. 2019.

[5] A. F. Bastos and S. Santoso, "Universal waveshape-based disturbance detection in power quality data using similarity metrics," *IEEE Trans. Power Del.*, vol. 35, no. 4, pp. 1779–1787, Aug. 2020, doi: 10.1109/TPWRD.2019.2954320.

[6] G. S. Chawda, A. G. Shaik, M. Shaik, S. Padmanaban, J. B. Holm-Nielsen, O. P. Mahela, and P. Kaliannan, "Comprehensive review on detection and classification of power quality disturbances in utility grid with renewable energy penetration," *IEEE Access*, vol. 8, pp. 146807–146830, 2020, doi: 10.1109/ACCESS.2020.3014732.

[7] Y. Liu, D. Yuan, Z. Gong, T. Jin, and M. A. Mohamed, "Adaptive spectral trend based optimized EWT for monitoring the parameters of multiple power quality disturbances," *Int. J. Electr. Power Energy Syst.*, vol. 146, Mar. 2023, Art. no. 108797.

[8] N. K. Buduru and S. B. Karanki, "Real-time power quality event monitoring system using digital signal processor for smart metering applications," *J. Electr. Eng. Technol.*, vol. 18, no. 4, pp. 3179–3190, Jul. 2023.

[9] M. Mishra, "Power quality disturbance detection and classification using signal processing and soft computing techniques: A comprehensive review," *Int. Trans. Electr. Energy Syst.*, vol. 29, no. 8, Aug. 2019, Art. no. e12008.

[10] S. Roy and S. Debnath, "PSD based high impedance fault detection and classification in distribution system," *Measurement*, vol. 169, Feb. 2021, Art. no. 108366.

[11] O. M. Olajide, "Power quality events classification on real-time voltage waveform using short time Fourier transform and Bayes classifier," *Int. J. Appl. Sci. Technol.*, vol. 8, no. 2, pp. 1–22, 2018.

[12] Y. Yu, W. Zhao, S. Li, and S. Huang, "A two-stage wavelet decomposition method for instantaneous power quality indices estimation considering interharmonics and transient disturbances," *IEEE Trans. Instrum. Meas.*, vol. 70, pp. 1–13, 2021.

[13] N. Ghaffarzadeh, "A new method for power quality events detection and classification using discrete wavelet transform and correlation coefficients," *Int. J. Ind. Electron. Control Optim.*, vol. 4, pp. 47–57, Oct. 2021.

[14] T. Chakravorti, N. R. Nayak, R. Bisoi, P. K. Dash, and L. Tripathy, "A new robust kernel ridge regression classifier for islanding and power quality disturbances in a multi distributed generation based microgrid," *Renew. Energy Focus*, vol. 28, pp. 78–99, Mar. 2019.

[15] S. Ranjbar, A. R. Farsa, and S. Jamali, "Voltage-based protection of microgrids using decision tree algorithms," *Int. Trans. Electr. Energy Syst.*, vol. 30, no. 4, Apr. 2020, Art. no. e12274.

[16] P. K. Ray, A. Mohanty, and T. Panigrahi, "Power quality analysis in solar PV integrated microgrid using independent component analysis and support vector machine," *Optik*, vol. 180, pp. 691–698, Feb. 2019.

[17] D. H. S. Nolasco, F. B. Costa, E. S. Palmeira, D. K. Alves, B. R. C. Bedregal, T. O. A. Rocha, R. L. A. Ribeiro, and J. C. L. Silva, "Wavelet-fuzzy power quality diagnosis system with inference method based on overlap functions: Case study in an AC microgrid," *Eng. Appl. Artif. Intell.*, vol. 85, pp. 284–294, Oct. 2019.

[18] S. Wang and H. Chen, "A novel deep learning method for the classification of power quality disturbances using deep convolutional neural network," *Appl. Energy*, vol. 235, pp. 1126–1140, Feb. 2019.

[19] S. Alshahrani, M. Abbod, and B. Alamri, "Detection and classification of power quality events based on wavelet transform and artificial neural networks for smart grids," *Saudi Arabia Smart Grid*, pp. 1–7, Dec. 2015. [Online]. Available: https://ieeexplore.ieee.org/abstract/document/7449296

[20] S. Khokhar, A. A. Mohd Zin, A. P. Memon, and A. S. Mokhtar, "A new optimal feature selection algorithm for classification of power quality disturbances using discrete wavelet transform and probabilistic neural network," *Measurement*, vol. 95, pp. 246–259, Jan. 2017.

[21] F. Zhao, D. Liao, X. Chen, and Y. Wang, "Recognition of hybrid PQ disturbances based on multi-resolution S-transform and decision tree," *Energy Eng.*, vol. 120, no. 5, pp. 1133–1148, 2023.

[22] I. S. Samanta, P. K. Rout, K. Swain, M. Cherukuri, and S. Mishra, "Dual-tree complex wavelet packet transform and regularized extreme learning machine-based feature extraction and classification of power quality disturbances," *Energy Syst.*, vol. 1, pp. 1–26, May 2023.

[23] D. A. Bashawyah and A. Subasi, "Power quality event detection using FAWT and bagging ensemble classifier," in *Proc. IEEE Int. Conf. Environ. Electr. Eng. IEEE Ind. Commercial Power Syst. Eur.*, Jun. 2019, pp. 1–5.

[24] P. Radhakrishnan, K. Ramaiyan, A. Vinayagam, and V. Veerasamy, "A stacking ensemble classification model for detection and classification of power quality disturbances in PV integrated power network," *Measurement*, vol. 175, Apr. 2021, Art. no. 109025.

[25] S. Mishra, R. K. Mallick, D. A. Gadanayak, and P. Nayak, "A novel hybrid downsampling and optimized random forest approach for islanding detection and non-islanding power quality events classification in distributed generation integrated system," *IET Renew. Power Gener.*, vol. 15, no. 8, pp. 1662–1677, Jun. 2021.

[26] Y. Wang, A. Raza, F. P. Mohammed, J. Ravishankar, and T. Phung, "Detection and classification of disturbances in the islanded micro-grid by using wavelet transformation and feature extraction algorithm," *J. Eng.*, vol. 18, pp. 5284–5286, 2019.

[27] A. Khandelwal and P. Neema, "State of art for power quality issues in PV grid connected system," in *Proc. Int. Conf. Nascent Technol. Eng. (ICNTE)*, Jan. 2019, pp. 1–4.

[28] O. Gandhi, D. S. Kumar, C. D. Rodríguez-Gallegos, and D. Srinivasan, "Review of power system impacts at high PV penetration Part I: Factors limiting PV penetration," *Sol. Energy*, vol. 210, pp. 181–201, Nov. 2020.

[29] S. Adak and H. Cangi, "The quality problems at low irradiance in the grid-connected photovoltaic systems," *Electr. Eng.*, vol. 1, pp. 1–13, Apr. 2024.

[30] P. Gupta and R. N. Mahanty, "An approach for detection and classification of transmission line faults by wavelet analysis," *Energy Educ. Sci. Technol.*, vol. 34, pp. 109–122, Aug. 2016.

[31] F. Xiao, T. Lu, M. Wu, and Q. Ai, "Maximal overlap discrete wavelet transform and deep learning for robust denoising and detection of power quality disturbance," *IET Gener., Transmiss. Distrib.*, vol. 14, no. 1, pp. 140–147, Jan. 2020.

[32] T. Guo, T. Zhang, E. Lim, M. López-Benítez, F. Ma, and L. Yu, "A review of wavelet analysis and its applications: Challenges and opportunities," *IEEE Access*, vol. 10, pp. 58869–58903, 2022.

[33] S. Prakash, S. Purwar, and S. R. Mohanty, "Adaptive detection of islanding and power quality disturbances in a grid-integrated photovoltaic system," *Arabian J. Sci. Eng.*, vol. 45, no. 8, pp. 6297–6310, Aug. 2020.

[34] T. P. Tun and G. Pillai, "Power quality event classification in distribution grids using machine learning," in *Proc. 56th Int. Universities Power Eng. Conf. (UPEC)*, Aug. 2021, pp. 1–6, doi: 10.1109/UPEC50034.2021.9548222.

[35] A. Vinayagam, V. Veerasamy, P. Radhakrishnan, M. Sepperumal, and K. Ramaiyan, "An ensemble approach of classification model for detection and classification of power quality disturbances in PV integrated microgrid network," *Appl. Soft Comput.*, vol. 106, Jul. 2021, Art. no. 107294.

[36] A. Vinayagam, M. L. Othman, V. Veerasamy, S. S. Balaji, K. Ramaiyan, P. Radhakrishnan, M. D. Raman, and N. I. Abdul Wahab, "A random subspace ensemble classification model for discrimination of power quality events in solar PV microgrid power network," *PLoS ONE*, vol. 17, no. 1, Jan. 2022, Art. no. e0262570.

[37] A. Yılmaz, A. Küçüker, and G. Bayrak, "Automated classification of power quality disturbances in a SOFC&PV-based distributed generator using a hybrid machine learning method with high noise immunity," *Int. J. Hydrogen Energy*, vol. 47, no. 45, pp. 19797–19809, May 2022.

[38] P. K. Dash, E. N. V. D. V. Prasad, R. K. Jalli, and S. P. Mishra, "Multiple power quality disturbances analysis in photovoltaic integrated direct current microgrid using adaptive morphological filter with deep learning algorithm," *Appl. Energy*, vol. 309, Mar. 2022, Art. no. 118454.

[39] D. Pattanaik, S. C. Swain, I. S. Samanta, R. Dash, and K. Swain, "Power quality disturbance detection and monitoring of solar integrated microgrid," *WSEAS Trans. POWER Syst.*, vol. 17, pp. 306–315, Oct. 2022.

[40] B. Eristi and H. Eristi, "Classification of power quality disturbances in solar PV integrated power system based on a hybrid deep learning approach," *Int. Trans. Electr. Energy Syst.*, vol. 2022, pp. 1–13, Jun. 2022.

[41] Y. S. U. Vishwanath, S. Esakkirajan, B. Keerthiveena, and R. B. Pachori, "A generalized classification framework for power quality disturbances based on synchrosqueezed wavelet transform and convolutional neural networks," *IEEE Trans. Instrum. Meas.*, vol. 72, pp. 1–13, 2023.

[42] J. Jiang, H. Wu, C. Zhong, Y. Cai, and H. Song, "A novel methodology for microgrid power quality disturbance classification using URPM-CWT and multi-channel feature fusion," *IEEE Access*, vol. 12, pp. 35597–35611, 2024, doi: 10.1109/ACCESS.2024.3350170.

SAIRAM MISHRA (Graduate Student Member, IEEE) received the B.Tech. degree in electrical engineering stream from Siksha 'O' Anusandhan University, Bhubaneswar, Odisha, India, in 2014, and the M.Tech. degree in power electronics and drives from the Indira Gandhi Institute of Technology, Sarang, Dhenkanal, Odisha, in 2018. He is currently pursuing the Ph.D. degree with the Department of Electrical Engineering, Siksha 'O' Anusandhan University. He is a Senior Research Fellow of the Council of Scientific and Industrial Research (CSIR), Government of India.

RANJAN KUMAR MALLICK (Member, IEEE) was born in India, in 1972. He received the bachelor's degree in electrical engineering from the Institution of Engineers, India, in 1996, the M.E. degree in power system engineering from VSSUT, Burla, Odisha, India, in 2001, and the Ph.D. degree from BPUT, Odisha, in 2013. He is currently a Professor with the Department of Electrical and Electronics Engineering, ITER, Siksha 'O' Anusandhan Deemed to be University, Odisha. He has 23 years of experience in teaching and research. His research interests include the application of power electronics, optimization techniques in power systems, economic load dispatch, the design and control of HVDC converters, load frequency controllers, optimal harmonic estimation in power systems, stability and protection of power systems, power quality, microgrid control, and protection along with machine learning and deep learning applications in power engineering.

PRAVATI NAYAK was born in India, in 1983. She received the bachelor's degree in electrical engineering, in 2004, the M.Tech. degree in power electronics and drives, in 2010, and the Ph.D. degree from Siksha 'O' Anusandhan (SOA) Deemed to be University, Odisha, India, in 2022. She is currently an Associate Professor with the Electrical Engineering Department, ITER, SOA Deemed to be University. She has a teaching experience of more than 17 years. Her research interests include microgrids, power systems protection, artificial intelligence, power quality, power electronics, machine learning, and deep learning applications in power systems.

THAIYAL NAAYAGI RAMASAMY (Senior Member, IEEE) received the bachelor's degree (Hons.) in electrical and electronics engineering from Bharathidasan University, Tiruchirappalli, India, in 2000, the master's degree in information technology from Alagappa University, Karaikudi, India, in 2003, the master's degree (Hons.) in power electronics and drives from Anna University, Chennai, India, in 2005, and the Ph.D. degree in electrical and electronic engineering from The University of Manchester, Manchester, U.K., in 2010. She is currently with Newcastle University in Singapore (NUiS), Singapore, where she is also the Director of Education, an Associate Professor, and a Senior Tutor of electrical power engineering. Her current research interests include renewable energy integration and applications in smart grids, power electronics for aerospace, electric vehicle applications, low-carbon electrical energy systems, and power electronic solutions to sustainability. She is a Life Member of ISTE and an Associate Editor of IEEE/CSEE JOURNAL OF POWER AND ENERGY SYSTEMS.

GAYADHAR PANDA (Senior Member, IEEE) received the Ph.D. degree from Utkal University, in 2007. He is currently a Professor with the Electrical Engineering Department, National Institute of Technology, Meghalaya, India. He has over 24 years of teaching and research experience. He has published more than 120 technical papers in national and international conference proceedings/journals and filed two patents. He has supervised eight Ph.D. students and currently supervising four Ph.D. scholars. He has led several research projects on the integration of renewable energy generation and power quality improvement. His work involves the design, implementation, and operation of ac/dc microgrids with interfacing converters that use digital signal processing, artificial intelligence techniques, and other novel control methods. His current research interests include automatic generation control, stability improvements using flexible alternating current transmission system devices, power quality, power electronic converters, and distributed power generation. He is a fellow of IE and a Life Member of ISTE. He was a recipient of the Power Medal, IE, India, for one of his research articles.